Polycation-siRNA nanoparticles can disassemble at the kidney glomerular basement membrane

Jonathan E. Zuckerman[1], Chung Hang J. Choi[1], Han Han, and Mark E. Davis[2]

Chemical Engineering, California Institute of Technology, Pasadena, CA 91125

Contributed by Mark E. Davis, January 17, 2012 (sent for review December 22, 2011)

Despite being engineered to avoid renal clearance, many cationic polymer (polycation)-based siRNA nanoparticles that are used for systemic delivery are rapidly eliminated from the circulation. Here, we show that a component of the renal filtration barrier—the glomerular basement membrane (GBM)—can disassemble cationic cyclodextrin-containing polymer (CDP)-based siRNA nanoparticles and, thereby, facilitate their rapid elimination from circulation. Using confocal and electron microscopies, positron emission tomography, and compartment modeling, we demonstrate that siRNA nanoparticles, but not free siRNA, accumulate and disassemble in the GBM. We also confirm that the siRNA nanoparticles do not disassemble in blood plasma in vitro and in vivo. This clearance mechanism may affect any nanoparticles that assemble primarily by electrostatic interactions between cationic delivery components and anionic nucleic acids (or other therapeutic entities).

pharmacokinetics | glomerulus

A major challenge with the use of small interfering RNA (siRNA) in mammals is their delivery to intracellular locations in specific tissues (1). The two most investigated approaches to siRNA delivery involve the combination of siRNA with cationic lipids (lipoplexes, liposomes, micelles) or cationic polymers (polyplexes) (2). Polymer-based siRNA delivery vehicles can be tuned to be nonimmunogenic, nononcogenic, nontoxic, and targeted (3). A targeted nanoparticle formulation of siRNA (not chemically modified) with a cationic, cyclodextrin-containing polymer (CDP)-based delivery vehicle (clinical version denoted CALAA-01) was shown to accumulate in human tumors and deliver functional siRNA from a systemic, i.v. infusion (4). This first-in-human study demonstrated the clinical potential for cationic polymer-based siRNA delivery systems.

Like most cationic polymer-based siRNA delivery systems (5–9), the siRNA/CDP nanoparticle is rapidly eliminated from circulation (shown in mice, monkeys, and humans) (10–12). In fact, polymer complexation often does not extend the circulation time of siRNA. The rapid clearance of these siRNA nanoparticles is puzzling because they are engineered to be above the size cutoff for single-pass clearance via renal filtration (13). In understanding the mechanism behind the rapid clearance of this type of cancer therapeutic, we can efficiently seek ways to increase their circulation time and, thus, enhance their anticancer efficacy (3).

We hypothesize that the paradoxical renal clearance of polycation-nucleic acid nanoparticles results from their binding and disassembly by components of the renal filtration barrier. Three key properties of such nanoparticles (diameters between 10 and 100 nm, positive zeta potentials, and electrostatically driven self-assembly) make them susceptible to this mechanism of clearance.

The renal filtration barrier, located within the glomerulus of the nephron, consists of three layers that must be traversed to enter the urinary space. These three layers are the glomerular endothelial fenestrations (≈100 nm) (14), the glomerular basement membrane (GBM), a 300-nm-thick connective tissue membrane rich in heparan sulfate (15) (pore size of 3 nm) (16) and the podocyte filtration slits (≈32 nm) (17). The renal filtration barrier, in its entirety, possesses an effective size cutoff of ≈10 nm, and is known to facilitate the rapid renal clearance of small molecules drugs and free siRNA.

Gold nanoparticles of up to 130 nm in size can cross the fenestrated glomerular endothelium but not the GBM (14). Therefore, we believe that siRNA nanoparticles of diameters of ≈100 nm in circulation can access the GBM and preferentially deposit there because of their positive surface charge. Once in the GBM, they are disassembled by the abundant negatively charged proteoglycans (e.g., heparan sulfate) present that structurally mimic the polyanionic charge of nucleic acids. After disassembly, their components are small enough to cross into the urinary space.

To test this hypothesis, we first demonstrate that siRNA nanoparticles do not disassemble in circulation. We then examine the distribution of siRNA nanoparticles in the kidney via microscopy methods and confirm that siRNA nanoparticle deposit and disassemble in the GBM. Finally, we analyze the kinetics of kidney transit by positron emission tomography (PET) studies and model the dynamic PET data by using insights derived from our kidney imaging experiments. The combination of these studies provides conclusive evidence to support our hypothesis.

Results

Nanoparticle Components Remain Assembled in Vivo and Will Assemble When Administered Separately in Vivo. The siRNA and polymer components of the nanoparticle (CDP/AD-PEG) assemble via electrostatic interactions into spherical 60- to 100-nm nanoparticles (Fig. 1) with an average zeta potential of 10.6 ± 1.5 mV.

Gel mobility shift assays were used to determine siRNA/CDP association in plasma (Fig. 2*A*). In these assays, the siRNA component of the nanoparticle is detected via ethidium bromide staining. Free siRNA present in a sample will migrate down the gel toward the anode. siRNA assembled within nanoparticles remains in the well or moves up toward the cathode. When incubated with 95% (vol/vol) mouse plasma the free siRNA band is broadened and migrates slower compared with siRNA in water, likely due to general electrostatic interaction with positive plasma components. siRNA has been shown to have a half-life of 1.2 h in 90% mouse plasma (18); therefore, all analysis from animal plasma were performed within 1 h of plasma collection to ensure that free siRNA present in the plasma sample could be visualized.

We first determined whether siRNA is released from the nanoparticles in circulation. Gel mobility shift assays on plasma from mice receiving injections of siRNA nanoparticles demonstrate that all of the siRNA in the samples was present in the well or migrated up toward the cathode with no evidence of free siRNA traveling toward the anode. These data suggest that the siRNA component of the nanoparticles is not displaced from the polymeric delivery components in vivo.

Furthermore, we determined whether the individual components of the nanoparticles, siRNA and polymers, could assemble in vivo. In these experiments, free siRNA was administered, then 1 min later, CDP/AD-PEG polymers were added. Plasma was

Author contributions: J.E.Z. and M.E.D. designed research; J.E.Z., C.H.J.C., and H.H. performed research; J.E.Z., C.H.J.C., H.H., and M.E.D. analyzed data; and J.E.Z., C.H.J.C., and M.E.D. wrote the paper.

The authors declare no conflict of interest.

Freely available online through the PNAS open access option.

[1]J.E.Z. and C.H.J.C. contributed equally to this work.

[2]To whom correspondence should be addressed. E-mail: mdavis@cheme.caltech.edu.

This article contains supporting information online at www.pnas.org/lookup/suppl/doi:10.1073/pnas.1200718109/-/DCSupplemental.

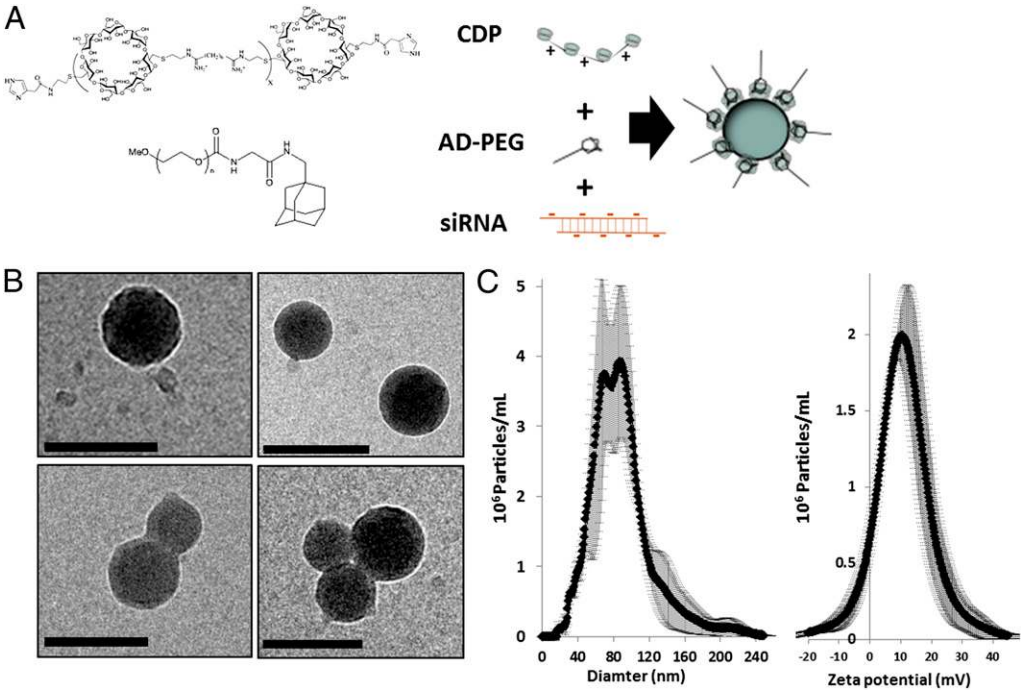

Fig. 1. Characterization of siRNA nanoparticles. (*A*) siRNA nanoparticles assemble because of electrostatic interactions between the cationic cyclodextrin containing polymer and the anionic siRNA. PEG provides steric stabilization and is bound to the particles via inclusion complex formation between its terminal adamantane (AD) modification and the cyclodextrin cup of the CDP. (*B*) Cryo-TEM images of siRNA nanoparticles revealed sub–100-nm spherical objects. (Scale bars: 100 nm.) (*C*) Nanoparticle tracking analysis of siRNA nanoparticle sizes and zeta potentials (error bars represent SD of three measurements, $n = 3$).

collected 1 min later. Plasma from mice receiving these sequential injections of individual nanoparticle components was analyzed. All of the siRNA in these samples remained in the well or traveled up toward the cathode, indicating its association with polymers. These results demonstrate that not only is the siRNA component of the nanoparticle not displaced from the polymer components, but that siRNA and polymer components will self-assemble in circulation.

Next, we confirmed that injection of free siRNA or polymer components alone could not result in nanoparticle-like bands on the gel. Analysis of plasma from animals receiving only siRNA demonstrated siRNA migrating down the gel toward the anode, confirming that free siRNA can be detected by the assay. Polymer components injected alone yielded no bands on the gel (except the nonspecific background band always present in plasma samples). These data confirm that the gel bands present in nanoparticle samples do not result from the association of siRNA or polymers with plasma components.

Finally, we induced nanoparticle disassembly in vivo to demonstrate that disassembled nanoparticles can be visualized via gel mobility shift assay. In vitro, we demonstrated that plasmid DNA could rapidly displaced siRNA from the nanoparticles by competitively binding to the positively charged polymer nanoparticle components (*SI Appendix*, Fig. S1). We hypothesized that injection of plasmid DNA 1 min after siRNA nanoparticle administration would induce nanoparticle disassembly in vivo and that free siRNA could be detected in these samples. Analysis of plasma from mice receiving sequential injections of siRNA nanoparticles

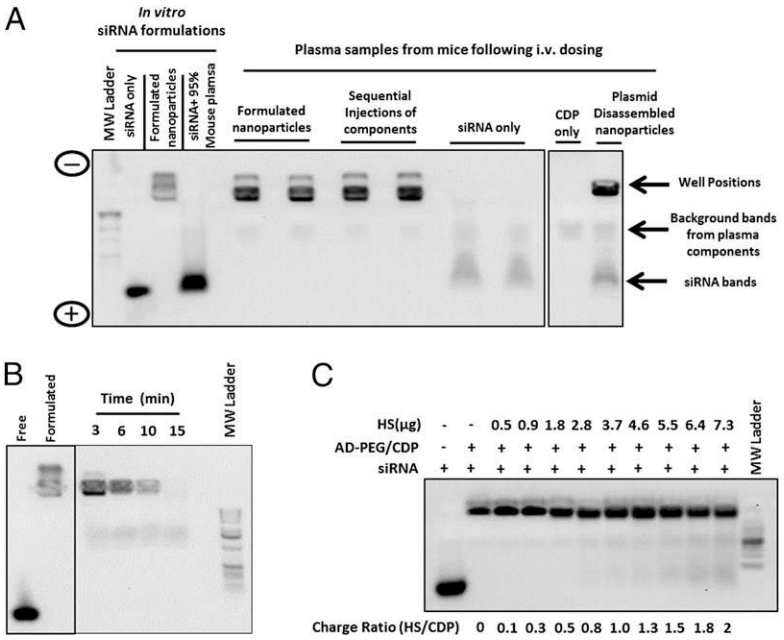

Fig. 2. Nanoparticle components remained associated and assembled in vivo but were disassembled by heparan sulfate. (*A–C*) Gel mobility shift assays demonstrated siRNA/CDP association. Free siRNA will migrate down the gel toward the anode, whereas siRNA/CDP nanoparticles remain in the wells or migrated toward the cathode. (*A*) In vitro siRNA formulations were formulated as indicated (formulated nanoparticles, siRNA+AD-PEG/CDP in H_2O) and incubated at 37 °C for 15 min. Plasma samples: Formulated nanoparticles, plasma from animals 3 min after injection of formulated siRNA+AD-PEG/CDP nanoparticles. Sequential injection of components, plasma from animals where free siRNA was injected and then 1 min later CDP/AD-PEG were injected; plasma was collected at 3 min after the first injection. siRNA or CDP only, plasma collected from animals 3 min after receiving injection of only siRNA or AD-PEG/CDP. Disassembled nanoparticles, plasma from animals where formulated siRNA nanoparticles were injected and then 1 min later an excess of ≈6 kb of plasmid DNA was injected, plasma was collected at 3 min after the first injection. All duplicate lanes are from independent animals. (*B*) Plasma samples from animals receiving formulated siRNA nanoparticles taken at the indicated time point after injection. (*C*) Gel mobility shift assays of siRNA nanoparticles in increasing amounts of heparan sulfate in 50% (vol/vol) mouse plasma. All plasma containing samples have a band of background staining that migrates at ≈5 kb as indicated in the figure.

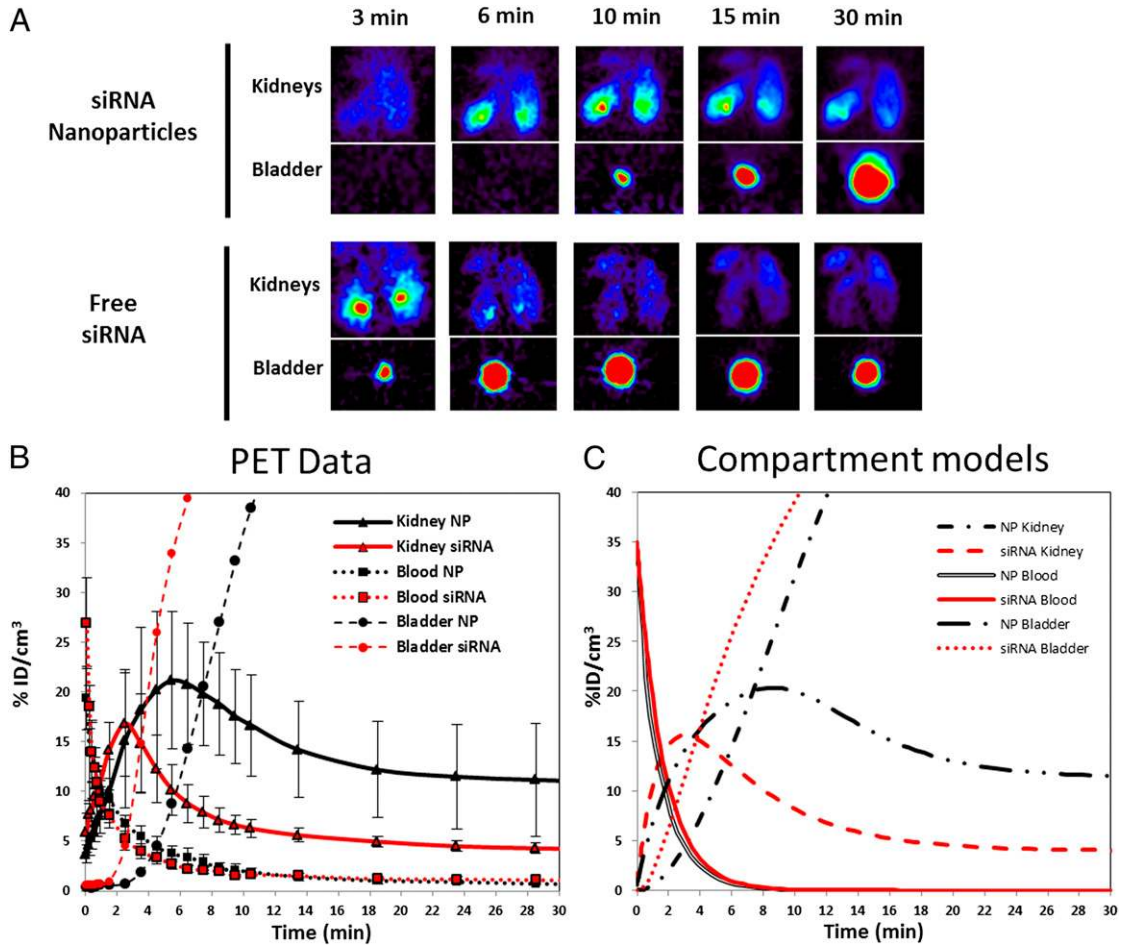

Fig. 3. Real-time PET imaging and compartment model of GBM-induced disassembly of siRNA nanoparticles. (*A*) Images of PET signal from kidneys and bladder of mice receiving free and nanoparticle-formulated ^{64}Cu-DOTA–labeled siRNA (data adapted from ref. 10). (*B*) Quantification of kidney, blood, and bladder ^{64}Cu-DOTA labeled siRNA intensities from PET studies [Error bars = SD, free siRNA $n = 4$, siRNA nanoparticles (NPs), $n = 5$]. (*C*) Computed results from compartment model of PET data for free siRNA (red) and siRNA nanoparticles (black).

and plasmid DNA confirmed our hypothesis. In these samples, the siRNA component of the nanoparticle was found to migrate down the gel toward the anode. These data demonstrate that disassembled nanoparticles can be detected via the gel mobility shift assays. Furthermore, they support our previous conclusion that siRNA is not displaced from the polymer in vivo by plasma components. Additionally, these data suggest that CDP can also self-assemble with plasmid DNA in vivo.

Gel mobility shift analysis on plasma samples taken at multiple time points after dosing of siRNA nanoparticles revealed siRNA remaining in the well for all time points (Fig. 2*B*). These data indicate that siRNA nanoparticles remain assembled over the entire circulation time of the particle.

Additionally, Oney et al. (19) have demonstrated that upon injection, the CDP can bind and completely neutralize the anticoagulant activity of i.v. doses of RNA aptamers targeting the coagulation factors IXa and Xa, suggesting that CDPs are capable of scavenging all free circulating RNA from plasma. Taken together, these data strongly suggest that rapid clearance of these siRNA nanoparticles is not from the result of disassembly in plasma.

Heparan Sulfate (HS) Disassembled siRNA Nanoparticle in Vitro. HS is a major constituent of the GBM and is responsible for its negative charge (15). HS is known to disassemble nucleic acid-containing, cationic polymer polyplexes (20). We confirmed that HS (extracted from bovine kidney) released siRNA from the nanoparticle at charge ratios (HS/CDP) above ±0.8 in 50% mouse plasma, whereas plasma alone could not (Fig. 2*C*). The amount of HS per mouse glomerulus is ≈2.5 μg (estimated from refs. 21 and 22) and 2,500 μg per kidney (≈10,000 glomeruli; ref. 23), a feasibly sufficient amount of HS to disassemble a single 10 mg/kg injection of siRNA nanoparticles (250 μg for a 25g mouse).

Dynamic PET Data Revealed Differences in Kidney Transit for siRNA Nanoparticles and Free siRNA. We used PET to track the dynamic, whole-body distribution of Cu^{64}-DOTA–labeled siRNA in mice and showed that siRNA in both free and nanoparticle forms demonstrated identical plasma half-lives and rapid clearance to the bladder (10). The only significant difference was in kidney transit: Compared with free siRNA, siRNA nanoparticles revealed delayed peak and increase in bulk kidney signal, and delayed transit from the kidney to the bladder for the siRNA nanoparticles (Fig. 3 *A* and *B*). The results from the dynamic PET data lead us to hypothesize that siRNA nanoparticles, but not free siRNA, transiently accumulate in the kidney before passing to the bladder.

siRNA Nanoparticles but Not Free siRNA Transiently Accumulated in Mouse Glomeruli After i.v. Administration. We hypothesized that the transient accumulation of the siRNA nanoparticles in the kidney suggested by our PET studies occurs in the glomerulus. We tested this hypothesis by using confocal microscopy to examine the distribution of free siRNA and siRNA nanoparticles in kidney during clearance. More than 90% of the administered nanoparticles have been shown to clear from circulation within 10 min and nearly

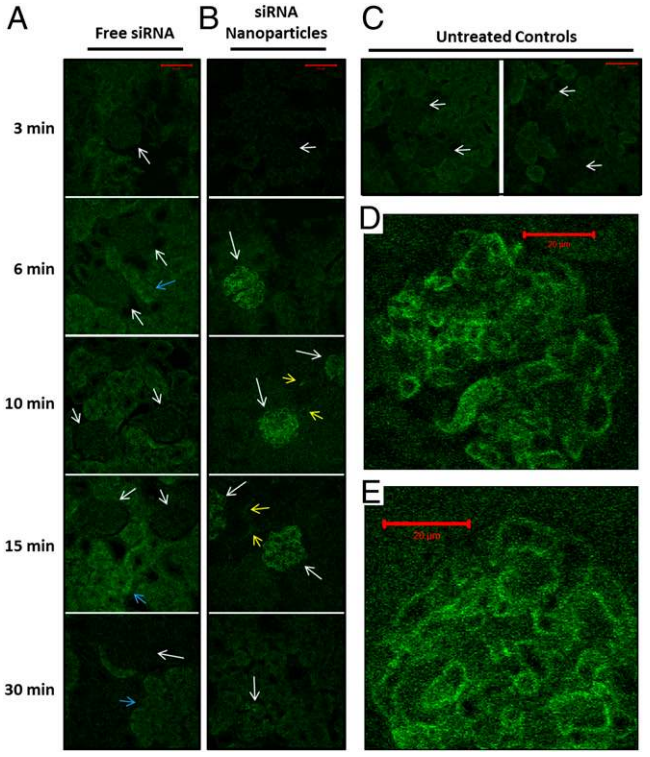

Fig. 4. siRNA nanoparticles, but not free siRNA, transiently accumulate in glomeruli after i.v. administration. Time course of confocal microcopy images of kidneys extracted from mice receiving free Cy3-labeled siRNA (*A*), Cy3-labled siRNA nanoparticles (*B*), or no treatment (*C*). Higher magnification images of glomeruli from 6 min (*D*) and 10 min (*E*) time points. White arrows indicate glomeruli positions, blue arrows indicate areas of tubular Cy3-signal accumulation, and yellow arrows indicate cy3 fluorescence in peritubule vasculature lining.

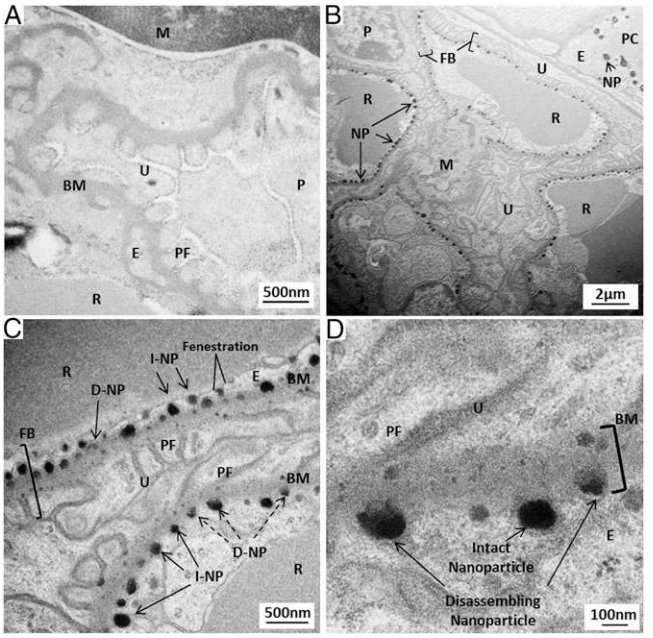

Fig. 5. Nanoparticles accumulate and disassemble at the kidney glomerular basement membrane. (*A*) Image of GBM from an animal receiving only free siRNA. (*B*) Low magnification EM image of glomerular capillaries from a mouse 10 min after i.v. administration of siRNA nanoparticles. (*C* and *D*) Higher magnification images of the GBM regions of these glomerular capillaries. BM, Basement membrane; E, Endothelial cell; FB, Filtration barrier, M, Mesangium, (I/D)-NP, (intact/disassembling) nanoparticle, P, podoyctes; PC, peritubule capillary; PF, podocyte foot process; R, Erythrocyte; U, Urinary space.

completely by 30 min (10). Therefore, we examined the distribution of siRNA nanoparticles in the kidney at time points between 3 and 30 min after i.v. injection. siRNA nanoparticles were formulated with 80% fluorescently labeled siRNA (Cy3). Formulation of nanoparticles with 80% Cy3-siRNA did not alter the size, charge, or stability of the nanoparticles.

After administration of free Cy3-labeled siRNA, fluorescence signal was observed to accumulate in renal tubules. The fluorescence signal in tubules increased until 10 min and then plateaued (Fig. 4*A*). No evidence for glomerular localization of Cy3-siRNA was observed in these animals at any time point. These observations are consistent with previous observations of free siRNA uptake by proximal tubule cells (24).

In striking comparison, strong Cy3 fluorescence signal localized to glomeruli was observed after administration of siRNA nanoparticles (Fig. 4*B*). This glomeruluar siRNA signal was observed first at 6 min after injection of the nanoparticles in ≈75% of glomeruli inspected. Close inspection of the glomeruli (Fig. 4 *D* and *E*) revealed Cy3 fluorescence localized to circular patterns that coincide with the lining the glomerular capillary walls (determined by position of red blood cells in the bright field image). These data demonstrate that the siRNA nanoparticles, but not free siRNA, accumulate in the glomerular capillary walls (the site of the GBM).

The glomerular siRNA nanoparticle Cy3 fluorescence intensity reached a maximum at 10 min, followed by attenuation at 15 min and 30 min. Observable glomeruli with fluorescent signal also decreased markedly at 15 min and were rarely detected at 30 min. These data indicate that siRNA nanoparticles only transiently accumulated within the glomerular capillary walls and ultimately exit the glomerulus. Visual examination of urine after nanoparticle administration revealed the highest Cy3 intensity at and 10 min after injection (*SI Appendix*, Fig. S2*A*), consistent with the assertion that siRNA accumulated in the glomerulus rapidly ends up in the urine, although Cy3 intensity in urine is similar after free siRNA administration (*SI Appendix*, Fig. S2*B*). Additionally, Cy3 was not readily cleaved from the siRNA molecule after 30 min in plasma (*SI Appendix*, Fig. S2*D*), indicating that any observed Cy3 fluorescence signals represents distribution of siRNA and not free Cy3.

Less Cy3 fluorescence was detected in tubules after siRNA nanoparticles administration than what was observed after free siRNA administration. These data suggest that the concentration of siRNA within the tubule lumen during clearance of the siRNA nanoparticles was consistently less than the concentration of siRNA when free siRNA was administered, despite the fact that both entities are clear from circulation at the same rate. These results support the notion that the renal filtration barrier is impeding the delivery of siRNA into the tubule system, preventing the higher concentrations required to drive higher levels of proximal tubule cell uptake.

Nanoparticles Deposit and Disassemble at the Kidney GBM. The confocal microscopy data demonstrated that the siRNA nanoparticles were accumulating in the lining of the glomerular vasculature. We used TEM to confirm that the siRNA signal in these locations resulted from siRNA in nanoparticle form accumulating specifically at the GBM (Fig. 5). We examined kidney tissue from mice 10 min after receiving free siRNA or siRNA nanoparticles because at this time point we observed maximal glomerular siRNA signals in both PET and confocal microscopy studies. We used uranyl acetate to detect the presence of nucleic acid nanoparticles in tissue sections because it preferentially binds to nucleic acids, including the siRNA within the nanoparticles (4, 20).

TEM analysis of kidney tissue after administration of free siRNA revealed typical appearing glomeruli. No darkly staining, globular structures indicative of nanoparticle morphology were observed within or near the GBM or any other structures in the kidney (Fig. 5*A*).

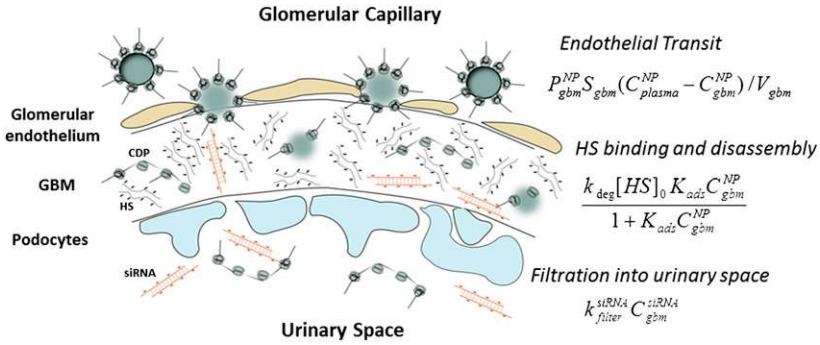

Fig. 6. Schematic of siRNA nanoparticle deposition and disassembly in the GBM with key modeling expressions highlighted. Nanoparticles cross through fenestrations in the glomerular endothelial cell lining and enter the GBM. Within the GBM, the nanoparticles are disassembled by the abundant heparan sulfate molecules. Once disassembled, the nanoparticle components can cross the remainder of the GBM and the podocyte filtration slits and enter the urinary space.

TEM analysis of kidney tissue after administration of siRNA nanoparticles revealed abundant, darkly staining, globular objects lining and within all visible GBMs, with sizes and shapes consistent with those of siRNA nanoparticles (Fig. 5 *B–D*). Most objects were localized to the lamina rara interna with some of the smaller objects localized to the limina rara externa, both are locations of anionic sites within the GBM (25). Additionally, some objects were observed within the glomerular endothelial fenestrations. No objects of this morphology were observed in the urinary space. The localization of the siRNA nanoparticles observed here matches the high intensity siRNA fluorescent signals along the glomerular capillary walls (site of the GBM) seen in the confocal microscopy studies. These data demonstrate that intact nanoparticles in circulation transit through the glomerular endothelial fenestrations and deposit within the GBM. Moreover, the absence of nanoparticles in the urinary space suggests that intact siRNA nanoparticles cannot cross the podocyte filtration slits of the renal filtration barrier.

Close inspection of these objects within the GBM revealed a subset of nanoparticle-sized objects with irregular borders and heterogeneous staining intensity (Fig. 5 *C* and *D*). The objects appeared to have lost their regularity and staining intensity in regions more closely associated with the GBM, implying the loss of some of their nucleic acid content compared with the uniform staining of intact siRNA nanoparticles. These data suggest that, upon GBM association, siRNA can be dissociated from the nanoparticle, i.e., nanoparticle disassembly was occurring at the GBM. Because there is no evidence for intact nanoparticles in the urinary space, these data also support our hypothesis that the transient nature of the GBM accumulation of siRNA nanoparticles observed in the confocal microscopy study stems from their disassembly at the GBM.

Some larger, darkly staining objects were also found within the endothelial cells lining the peri-tubule capillaries after siRNA nanoparticle treatment (*SI Appendix*, Fig. S3 *A* and *B*), consistent in morphology with unpackaging nanoparticles within endosomes (20). These data are consistent with the results from our confocal microscopy study, where we observed some non-glomerular renal vessels with appreciable fluorescence signal in their walls in tissue from mice receiving siRNA nanoparticle treatment. Renal peri-tubule endothelial cell uptake of pegylated gold nanoparticles has been observed (14) and may be a generalized phenomenon for nanoparticle systems.

Compartment Modeling of Kidney Transit Revealed how siRNA Nanoparticle Accumulation and Disassembly at the GBM Could Yield the Kinetics Observed in the PET Experiments. Because noninvasive, real-time monitoring of siRNA nanoparticle behavior at the microscopic level was not possible, we developed a mathematical compartment model of kidney transit to correlate our microscopic observations with the bulk kidney signal from the dynamic PET experiments (Fig. 3*C* and *SI Appendix*, *SI Text*).

Kinetic parameters for a model describing the transit of free siRNA through the kidney were derived from anatomic properties of the kidney and by fitting the PET data for free siRNA ("free siRNA model"). Based on our imaging data, two additional expressions were incorporated into the free siRNA model to create the "siRNA nanoparticle model": (*i*) an expression to model the binding and disassembly of the nanoparticles within the GBM, and (*ii*) an expression for peri-tubule endothelial cell uptake. All parameter values were fixed to those derived in the free siRNA model, except those pertaining to the two nanoparticle specific expressions (e.g., binding constant of nanoparticle on the GBM and rate of disassembly of nanoparticle) that were determined by fitting the PET data for siRNA nanoparticles. Assimilation of these two expressions into the nanoparticle model allowed us to model the key differences in the PET pharmacokinetics data between free siRNA and siRNA nanoparticles as they pass through the kidney—the delayed bladder accumulation, delayed peak kidney accumulation, and persistent kidney signal for the siRNA nanoparticle experiments.

Kinetic parametric sensitivity analyses of both models confirmed that both GBM and endothelial cell expressions of the nanoparticle model are required to reproduce the observed kidney dynamics of siRNA nanoparticles in the PET data. No arbitrary choice of parameters in the free siRNA model could delay the peak kidney accumulation to fit the nanoparticle PET data, except through the addition of the expression for GBM binding and disassembly in the nanoparticle model. Therefore, mathematical compartment modeling demonstrate that the glomerular accumulation and disassembly of the siRNA nanoparticles revealed by imaging data (confocal and TEM) could be responsible for the dynamics observed in our PET experiments. Additionally, this analysis suggests that siRNA dissociated from nanoparticles in circulation could not recapitulate the dynamics observed in the kidney.

Discussion

Here, we have elucidated a unique mechanism of nanoparticle disassembly in vivo (Fig. 6). We have demonstrated that siRNA/CDP nanoparticles remain assembled and that their individual components can even self-assemble in circulation. Moreover, using microscopy, we have conclusively demonstrated that siRNA/CDP nanoparticles transiently accumulate in and can be disassembled by the GBM. Finally, using compartment modeling, we illustrated how our microscopic observation of GBM accumulation and disassembly could feasibly result in the bulk dynamics observed by PET, whereas disassembly in circulation could not.

To date, the rapid clearance of siRNA-cationic polymer nanoparticles has been ascribed to instability in circulation and reticuloendothelial system uptake (5–7, 9, 10). Extracellular matrix-mediated disruption of cationic nucleic acid polyplexes within liver sinusoids has also been reported (26). Although our findings do not exclude these alternate explanations for other nanoparticle delivery systems, they reveal another clearance mechanism applicable to a general class of nanoparticles with the following characteristics: (*i*) ≈100 nm or smaller in hydrodynamic radius, (*ii*) positive in zeta potential, and (*iii*) held together primarily by electrostatic interaction.

Because the siRNA nanoparticles presented here not only remain assembled in plasma, but their individual components self-assemble in vivo, it is unlikely that the components of the nanoparticle prefer to exist freely in circulation. These data also

suggest that even if the nanoparticles were disassembled at other locations in the body, the individual components would reassemble in circulation. Thus, only nanoparticle disassembly at that GBM would allow transit of the nanoparticle components into the urine. In fact, the siRNA nanoparticle components are found to be mostly assembled in urine after excretion (*SI Appendix*, Fig. S2*C*), suggesting that particles re-form in the urine after GBM disassembly and filtration.

Therefore, GBM-mediated nanoparticle disassembly is responsible for the rapid clearance of the siRNA/CDP nanoparticles. This phenomenon is likely generalizable to most cationic polymer-based nucleic acid delivery systems, or any other delivery vehicles that self-assemble because of electrostatic interactions. For example, 93-nm DNA/PEI polyplexes have been observed to filter through the GBM after direct injection into the renal artery (27), and both Cationic polymers alone (28) and positively charged ferritin nanoparticles (29) have been shown to bind to the GBM after i.v. injection.

Avoiding GBM disassembly will be a key design criterion for future nucleic acid delivery vehicles and other nanoparticle systems assembled via electrostatic interactions. Future nanoparticle therapeutic development could be facilitated via heparan sulfate stability studies during design. Furthermore, creation of particles with negative zeta potentials may allow avoidance of the GBM due to charge repulsion. Our study of 20- to 170-nm negatively charged PEGylated gold particles did not reveal any particle deposition in the GBM for nanoparticles of any size (14). Finally, this mechanism of clearance could be used to tune the pharmacokinetics of nanoparticles based on their stability to heparan sulfate disassembly, thereby providing a convenient mechanism for more rapid clearance, when desirable, for particles >10 nm such as imaging agents.

Materials and Methods

Complete details of materials and methods are found in *SI Appendix*.

siRNA Nanoparticle Formulation. siRNA nanoparticles were formed by using CDP and AD-PEG as described in ref. 30 (precomplexation).

NTA. NTA measurements were performed with a NanoSight NS500 (NanoSight), equipped with a 405-nm laser.

Animal Studies. Six- to nine-week-old, female BALB/c mice (The Jackson Laboratory) were used for all studies.

In Vivo siRNA/CDP Assembly/Disassembly Assays. Experiment 1: Free siRNA was injected at 10 mg/kg dose via tail vein. Experiment 2: siRNA nanoparticles were injected at 10 mg/kg via tail vein. Experiment 3: Free siRNA was injected at 10 mg/kg, 1 min later CDP/AD-PEG components were injected at a ±3 charge ratio of the injected siRNA. Experiment 4: CDP/AD-PEG was injected at nanoparticle equivalent concentration. Experiment 5: siRNA nanoparticles were injected at 2.5 mg/kg; 1 min later, 10 mg/kg plasmid DNA was injected. Blood collection for all three experiments was performed via saphenous vein bleed 3 min after the first injection.

Electron Microscopy. Samples were visualized in a Techni T12 Cryo-electron microscope (FEI) or TF30UT transmission electron miscroscope (FEI).

Confocal Microscopy. Images were obtained on a Zeiss LSM 510 inverted confocal scanning microscope (with a Plan Neofluar 40×/0.75 objective).

Micro-PET/CT Imaging. Micro-PET imaging was performed as described (10).

Compartment Modeling. Model variables and parameters are defined in *SI Appendix, SI Text*.

ACKNOWLEDGMENTS. We thank Paul Webster (House Ear Institute) for providing equipment for TEM sample preparation and Carol M. Garland (California Institute of Technology) and Dr. Alasdair McDowall (California Institute of Technology) for help obtaining electron microscopy images. This work benefited from the use of the California Institute of Technology Materials Science TEM facility, which is partially supported by the Materials Research Science & Engineering Center Program of the National Science Foundation under Award DMR-0520565. We thank Derek W. Bartlett and Isabel J. Hildebrandt for performing the PET experiments and Devin Wiley for reading the manuscript and discussion. This work was supported by National Cancer Institute Grant CA119347 and Sanofi-Aventis. J.E.Z. is also supported by the California Institute of Technology-University of California, Los Angeles Joint Center for Translational Medicine.

1. Castanotto D, Rossi JJ (2009) The promises and pitfalls of RNA-interference-based therapeutics. *Nature* 457:426–433.
2. de Fougerolles A, Vornlocher HP, Maraganore J, Lieberman J (2007) Interfering with disease: A progress report on siRNA-based therapeutics. *Nat Rev Drug Discov* 6: 443–453.
3. Davis ME, Chen ZG, Shin DM (2008) Nanoparticle therapeutics: An emerging treatment modality for cancer. *Nat Rev Drug Discov* 7:771–782.
4. Davis ME, et al. (2010) Evidence of RNAi in humans from systemically administered siRNA via targeted nanoparticles. *Nature* 464:1067–1070.
5. de Wolf HK, et al. (2007) Effect of cationic carriers on the pharmacokinetics and tumor localization of nucleic acids after intravenous administration. *Int J Pharm* 331: 167–175.
6. Malek A, et al. (2009) In vivo pharmacokinetics, tissue distribution and underlying mechanisms of various PEI(-PEG)/siRNA complexes. *Toxicol Appl Pharmacol* 236: 97–108.
7. Merkel OM, et al. (2009) Stability of siRNA polyplexes from poly(ethylenimine) and poly(ethylenimine)-g-poly(ethylene glycol) under in vivo conditions: Effects on pharmacokinetics and biodistribution measured by Fluorescence Fluctuation Spectroscopy and Single Photon Emission Computed Tomography (SPECT) imaging. *J Control Release* 138:148–159.
8. Merkel OM, et al. (2010) Triazine dendrimers as nonviral vectors for in vitro and in vivo RNAi: The effects of peripheral groups and core structure on biological activity. *Mol Pharm* 7:969–983.
9. Gao S, et al. (2009) The effect of chemical modification and nanoparticle formulation on stability and biodistribution of siRNA in mice. *Mol Ther* 17:1225–1233.
10. Bartlett DW, Su H, Hildebrandt IJ, Weber WA, Davis ME (2007) Impact of tumor-specific targeting on the biodistribution and efficacy of siRNA nanoparticles measured by multimodality in vivo imaging. *Proc Natl Acad Sci USA* 104:15549–15554.
11. Heidel JD, et al. (2007) Administration in non-human primates of escalating intravenous doses of targeted nanoparticles containing ribonucleotide reductase subunit M2 siRNA. *Proc Natl Acad Sci USA* 104:5715–5721.
12. Ribas A, et al. (2010) Systemic delivery of siRNA via targeted nanoparticles in patients with cancer: Results from a first-in-class phase I clinical trial. *J Clin Oncol* 28:3022.
13. Choi HS, et al. (2007) Renal clearance of quantum dots. *Nat Biotechnol* 25:1165–1170.
14. Choi CH, Zuckerman JE, Webster P, Davis ME (2011) Targeting kidney mesangium by nanoparticles of defined size. *Proc Natl Acad Sci USA* 108:6656–6661.
15. Kanwar YS, Farquhar MG (1979) Presence of heparan sulfate in the glomerular basement membrane. *Proc Natl Acad Sci USA* 76:1303–1307.
16. Ogawa S, et al. (1999) High-resolution ultrastructural comparison of renal glomerular and tubular basement membranes. *Am J Nephrol* 19:686–693.
17. Lahdenkari A-T, et al. (2004) Podocytes are firmly attached to glomerular basement membrane in kidneys with heavy proteinuria. *J Am Soc Nephrol* 15:2611–2618.
18. Bartlett DW, Davis ME (2007) Effect of siRNA nuclease stability on the in vitro and in vivo kinetics of siRNA-mediated gene silencing. *Biotechnol Bioeng* 97:909–921.
19. Oney S, et al. (2009) Development of universal antidotes to control aptamer activity. *Nat Med* 15:1224–1228.
20. Mishra S, Heidel JD, Webster P, Davis ME (2006) Imidazole groups on a linear, cyclodextrin-containing polycation produce enhanced gene delivery via multiple processes. *J Control Release* 116:179–191.
21. Comper WD, Lee AS, Tay M, Adal Y (1993) Anionic charge concentration of rat kidney glomeruli and glomerular basement membrane. *Biochem J* 289:647–652.
22. Westberg NG, Michael AF (1970) Human glomerular basement membrane. Preparation and composition. *Biochemistry* 9:3837–3846.
23. Takemoto M, et al. (2002) A new method for large scale isolation of kidney glomeruli from mice. *Am J Pathol* 161:799–805.
24. Molitoris BA, et al. (2009) siRNA targeted to p53 attenuates ischemic and cisplatin-induced acute kidney injury. *J Am Soc Nephrol* 20:1754–1764.
25. Kanwar YS, Farquhar MG (1979) Anionic sites in the glomerular basement membrane. In vivo and in vitro localization to the laminae rarae by cationic probes. *J Cell Biol* 81: 137–153.
26. Burke RS, Pun SH (2008) Extracellular barriers to in Vivo PEI and PEGylated PEI polyplex-mediated gene delivery to the liver. *Bioconjug Chem* 19:693–704.
27. Foglieni C, et al. (2000) Glomerular filtration is required for transfection of proximal tubular cells in the rat kidney following injection of DNA complexes into the renal artery. *Gene Ther* 7:279–285.
28. Andrews PM, Bates SB (1985) Dose-dependent movement of cationic molecules across the glomerular wall. *Anat Rec* 212:223–231.
29. Bennett KM, et al. (2008)) MRI of the basement membrane using charged nanoparticles as contrast agents. *Magn Reson Med* 60:564–574.
30. Bartlett DW, Davis ME (2007) Physicochemical and biological characterization of targeted, nucleic acid-containing nanoparticles. *Bioconjug Chem* 18:456–468.